Frontiers Med. Biol. Engng, Vol. 7, No. 1, pp. 45–70 (1995)

Original paper

A compartmental brain model for chemical transport and CO_2 controlled blood flow

SHAUL SOREK,[1,*] ALEX YAKIREVICH[1] and MOSHE FEINSOD[2]

[1] *Ben-Gurion University of the Negev, J. Blaustein Institute for Desert Research, Sede Boqer Campus 84990, Israel*

[2] *Department of Neurosurgery, Technion, Haifa 32000, Israel*

Received 8 March 1995; accepted 10 August 1995

Abstract—A compartmental transport model is developed, capable of predicting the evolution of CO_2, HCO_3^- and H^+ in the cerebrovascular system. In the model, the transport of these components is simulated at a subset of three compartments: cerebrospinal fluid (CSF), capillary–choroid plexus and brain tissue, belonging to a seven compartmental assembly representing the entire brain. The remaining ones are: artery, vein, venous sinus and jugular bulb. The model accounts for advection associated with non-steady perfusion fluxes across semi-pervious boundaries. Pressures, associated with perfusion, are solved in the seven-compartment model. The three-compartment transport model also takes into account changes in compartmental volume due to displacement of its boundaries, diffusion through boundaries and rate of generation of substances by chemical reactions. A first-order reaction rate is assumed in the CSF compartment. A parameter estimation method is then developed to assess boundary diffusivities from time-averaged observed values of perfusion pressure, tension of carbon dioxide, pH values, and concentration of free hydrogen and bicarbonate ions. An equation of state describing the regulation of flow from arteries to capillaries, as a function of CO_2 tension in the CSF, is then suggested. Upon solving all coupled mass balance equations, and for a pre-evaluated perfusion pressure in the artery and capillary compartments, one can estimate the change in arteries to capillaries conductance at every time step. Boundary diffusivities between the capillary, cerebrospinal fluid and brain tissue compartments, were estimated. A sensitivity analysis proves the consistency between model predictions and available clinical observations, this, in terms of the influence of the parameter associated with CO_2 metabolic rate on CO_2 tension. It was shown that decrease of this tension caused an abrupt pressure fall at the first instant which later increased to an asymptotic value. This, however, was not evident in the capillaries at which pressure slightly falls and then remains constant.

Key words: compartmental system; non-steady perfusion fluxes; compliance; conductance; diffusion; advection; chemical reactions; molecular CO_2; bicarbonate ion; hydrogen ion; parameter estimation; sensitivity analysis.

*Also affiliated with Mechanical Engineering Department, Ben-Gurion University of the Negev, Beer Sheva, Israel.

1. INTRODUCTION

Experiments [1] showed that the flow of blood from the *arteries* to the *capillaries* within the cerebrovascular system is controlled by changes in the concentration of CO_2 within the brain tissue. In order to investigate changes in this flow in response to changes in CO_2 concentration, a model that simulates chemical transport and blood flow in the brain system was constructed. Following earlier works by the authors [2–5], a multicompartmental model was selected for this purpose. In such a model each part of the brain, identified by a certain function that it fulfills, is simulated as a compartment characterized by unique values of time-dependent variables, such as pressure and concentration of considered chemical components. Adjacent compartments interact with each other, enabling flow of fluids (here blood) and chemicals (e.g. CO_2 dissolved in the blood) to be transported across intercompartmental boundaries. Mechanisms of species transport include perfusion with the blood and molecular diffusion. In addition, various chemical reactions involving CO_2, HCO_3^- and H^+ take place, affecting their concentration. A model of this kind is often referred to as a *fully mixed, lumped parameter model.*

In Sorek *et al.* [3] a detailed description is given with regard to their choice of compartmental model, the chosen resistances and compliances and the role of these parameters in relation to physiology. Following this, we use the same model composed of seven compartments to simulate the following brain parts: artery (A), capillary–choroid plexus (C), venous (V), venous sinus (S), jugular bulb (J), cerebrospinal fluid (F) and brain tissue (B). In this model, for example, the resistances R_{CB}, R_{CF} and R_{FB} are identified as the blood–brain barrier, the blood–CSF barrier and the CSF–brain barrier, respectively. Displacement is introduced in terms of compliances. This, for example, allows the choroid plexus to convey pulsations to the CSF system [6].

In the model investigated here, it is assumed that a single (averaged) incompressible fluid flows through the various compartments that simulate the cerebral system. The mathematical model is comprised of mass and momentum balance equations for the fluid and mass balance equations for each of the chemical substances influencing the CO_2 transport.

2. THEORETICAL DEVELOPMENT

2.1. The lumped parameter flow model

Figure 1 shows three adjacent compartments, (i), (j) and (n), separated by common boundaries which permit fluid to leak through them, from (i) into (n) and from (n) into (j). They also allow components dissolved in the fluid to be transported across the boundary. The solute is transported through any boundary by two mechanisms: advection with the fluid, commonly referred to as transport by *perfusion*, and molecular diffusion. The boundary itself acts as a semi-pervious membrane which can be displaced in response to pressure changes in the adjacent compartments. This displacement produces changes in the volume of each compartment. We use the term

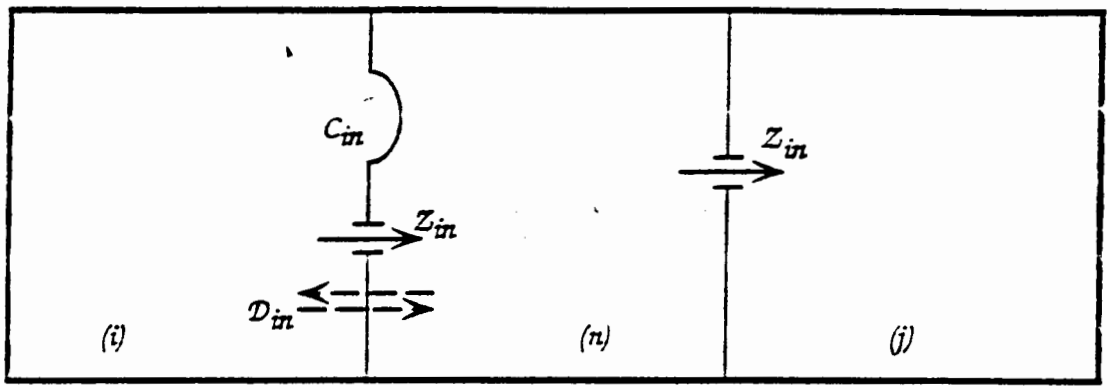

Figure 1. Three compartments with flow through common boundaries with conductances Z(—|↑|—), compliances C(⌒) and transport D(⇄) coefficients.

compliance to describe the relation between the change in a compartment's volume to the change in the pressure difference across it.

For a fluid of constant density, ρ, the mass balance for the (n)th compartment expressed by

$$\sum_{i=1}^{I_{(n)}} q_{in} - \sum_{j=1}^{J_{(n)}} q_{nj} + Q_{(n)} = \frac{dV_n}{dt}, \tag{1}$$

where $I_{(n)}$ and $J_{(n)}$ denote the number of compartments from which flow enters the (n)th compartment, and leaves it, respectively; q_{in} and q_{nj} denote the fluxes from the (i)th compartment into the (n)th one and from the (n)th one to the (j)th one, respectively; $Q_{(n)}$ denotes the fluid sources in the (n)th compartment and V_n denotes the volume of compartment (n). The compartmental volume is affected by the rigidity of the displaced boundary in response to changes in the pressure difference $P_{mn} = (P_m - P_n)$ across the mutual boundary between compartments (m) and (n).

Within the cerebral system, differences in elevation, H, are small. Hence, we may assume that between two compartments, m and n, we have

$$P_{mn} \equiv (P_m - P_n) \gg \rho g(H_m - H_n), \tag{2}$$

where g denotes the gravity acceleration.

The flux through a semi-pervious boundary between two compartments is proportional to the piezometric (≡ hydraulic) head difference between them. However, in view of (2), we assume that the flux is proportional to the pressure difference, i.e.

$$q_{in} = Z_{in} P_{in}, \tag{3}$$

where Z_{in} is called the conductance of the boundary between the (i)th and (n)th compartments. The rate of change in V_n appearing in (1) is expressed by

$$\frac{dV_n}{dt} = \sum_{m=1}^{M_{(n)}} \frac{dV_n}{dP_{mn}} \frac{dP_{mn}}{dt} = \sum_{m=1}^{M_{(n)}} C_{mn} \frac{dP_{mn}}{dt}, \tag{4.1}$$

where C_{mn} denotes the value of the compliance of the (n)th compartment due to the displacement of its boundary with the (m)th one and $M_{(n)}$ is the number of boundaries of compartment (n) that are associated with a compliance.

The compliance, C_{mn}, is defined by

$$C_{mn} = \frac{\mathrm{d}V_n}{\mathrm{d}P_{mn}}. \tag{4.2}$$

In view of (3) and (4), we can now rewrite (1) in the form

$$Q_{(n)} = -\sum_{i=1}^{I_{(n)}} Z_{in} P_{in} + \sum_{j=1}^{J_{(n)}} Z_{nj} P_{nj} + \sum_{m=1}^{M_{(n)}} C_{mn} \frac{\mathrm{d}P_{mn}}{\mathrm{d}t}. \tag{5}$$

In general, the various Z_{in}'s and C_{mn}'s are assumed constant. In this paper (as in earlier papers by the authors [3–5]), these coefficients are allowed to vary as functions of time, e.g. in the form of a step function in time, say, in response to illness. As will be shown in the section below, the conductance between the arteries and the capillaries depends on the arterial CO_2 tension.

Equation (5) constitutes a set of n equations, one for each of the n compartments, in the n unknown pressures, P_n. It does not incorporate osmotic pressure falls, an additional term which reduces the total pressure, influential especially when considering transport of proteins and regarded as the colloidal osmotic pressure. In our model the osmotic pressure associated with the CO_2, HCO_3^- and H^+ ions is by many orders less than the one generated by proteins and can be, accordingly, neglected. Furthermore, the osmotic values of blood and CSF are similar, and therefore do not produce any osmotic pressure fall.

2.2. *Transport of chemical components*

Our next objective is to formulate the mass balance equation for the chemical components transported through the compartmental system.

A detailed literature survey on the effect of changes in arterial CO_2 tension on cerebral blood flow is documented in Greenberg *et al.* [1]. In that work, a mathematical model is developed that relates the cerebral blood flow control to changes of CO_2 tension in the arteries (P_aCO_2). Greenberg's model of the controlled perfusion in the brain system is composed of three compartments: capillaries (blood), cerebral extracellular fluid and cerebral intracellular fluid. His model is based on the assumption of rigid compartmental walls and constant perfusions blood pressure.

In what follows, we present a modification and an extension of Greenberg's model. The extra/intra cellular fluid compartments are subject to the same pressure, hence they are lumped into one brain tissue compartment. We relax the assumption of rigid walls by introducing compliances and by solving the perfusion pressure for a non-steady system.

The general layout, composed of a seven-compartment system, is shown in Fig. 2. This general system was developed by Sorek *et al.* [3] to evaluate changes in the

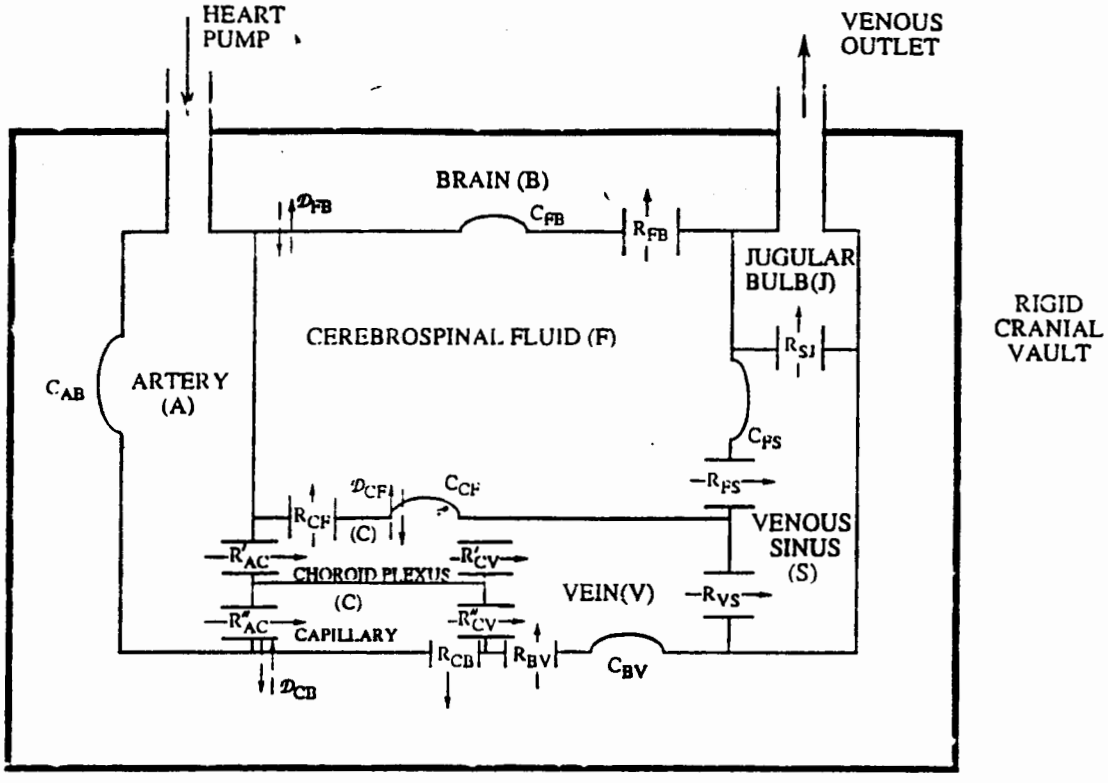

Figure 2. Cerebral seven-compartmental system for perfusion pressure and transport processes.

cerebral perfusion pressure. Figure 3 shows the transport as conceived by Davson [7] and Greenberg *et al.* [1]. Our aim is to include in the model the regulation of arterial to capillary conductance as a function of CO_2 pressure associated with perfusion flux and changes in compartment volume related to boundary compliance.

Following the discussion of Greenberg *et al.* [1], we focus our attention on the hydration reaction that takes place in the physiologic fluid circulating through the cerebrovascular system

$$CO_2 + H_2O \underset{k_R}{\overset{k_F}{\rightleftharpoons}} HCO_3^- + H^+. \tag{6}$$

This chemical reaction influences the transport of dissolved CO_2 and will thus be considered in the model. The coefficients k_F and k_R are the forward and reverse rate constants, respectively.

In view of (6), the three chemical species that are involved in controlling the block flow are: molecular carbon dioxide (CO_2), bicarbonate ion (HCO_3^-) and the hydrogen ion (H^+).

In developing the transport equations, we write a mass balance equation for each of these substances, using the notation: $l = 1$ for CO_2, $l = 2$ for HCO_3^- and $l = 3$ for H^+.

For the mixed cell idealization considered here, with no external sources or sinks of the components, the mass balance for the l substance in compartment n, is expressed

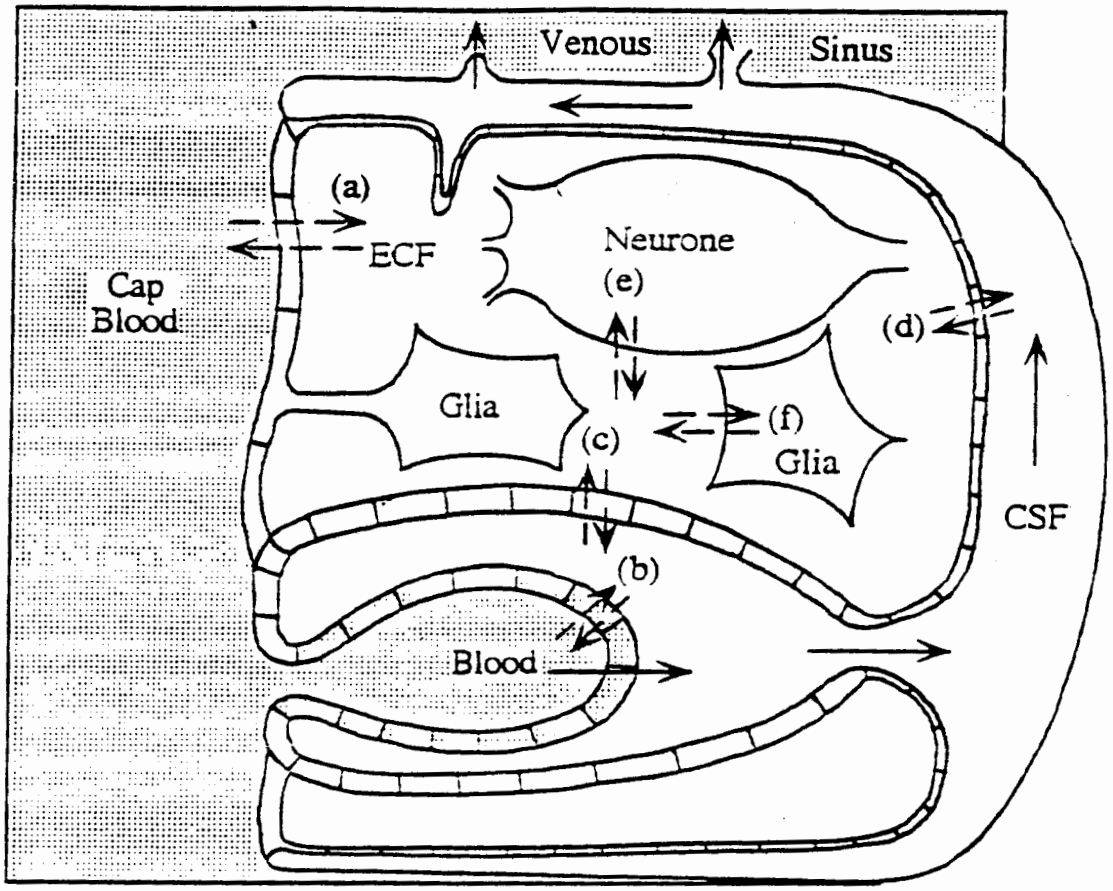

Figure 3. Schematic of the brain model compartments showing both fluid flow (solid arrows) and diffusion (broken arrows) between compartments. Transport is (a) between extracellular fluid (ECF) and capillary blood, (b) between the capillary blood and cerebrospinal fluid (CSF), (c, d) between the CSF and ECF, (e, f) between the cells (glia and neurons) and the ECF (modified from Davson [7] and after Greenberg *et al.* [1]).

by

$$\frac{\mathrm{d}}{\mathrm{d}t}(c_n^l V_n) = \sum_{i=1}^{I_{(n)}} c_{i(n)}^l q_{in} - c_n^l \sum_{j=1}^{J_{(n)}} q_{nj} + \sum_{k=1}^{K_{(n)}} J_{kn}^l + R_n^l, \tag{7}$$

where c_n^l is the concentration, i.e. mass of species l *per unit volume of compartment* n, R_n^l denotes the rate of production of the lth substance by chemical reaction in the nth compartment, $c_{i(n)}^l$ is the concentration of species l in cell i entering cell n, J_{kn}^l is the flux by diffusion of the substance l from compartment k into cell n through their common boundary (a total of $K_{(n)}$ such boundaries). The perfusion fluxes, q_{in} and q_{nj}, are related to the pressure difference by (3). As the pressure fluctuates, these advective fluxes, that carry solutes, also fluctuate in magnitude. In most existing models, these fluxes are assumed constant. For example, the flux from the arteries to the capillaries, which affects the corresponding solute transport, varies in the range of

around 5% (for an average of 750 mm/min [4]). The diffusive flux is expressed by

$$J^l_{kn} = D^l_{kn}\left(c^l_{k(n)} - c^l_n\right), \tag{8}$$

where D^l_{kn} is a coefficient that is related to the diffusivity and 'thickness' of the boundary, thus regarded as *boundary diffusivity*. By expanding the first term of (7) and in view of (4.1), we obtain

$$\frac{\mathrm{d}}{\mathrm{d}t}\left(c^l_n V_n\right) = \left[\sum_{m=1}^{M_{(n)}} C_{mn}\frac{\mathrm{d}P_{mn}}{\mathrm{d}t}\right] c^l_n + \overline{V}_n \frac{\mathrm{d}c^l_n}{\mathrm{d}t}. \tag{9}$$

By integrating (4.2), we use the symbol $\overline{V}_n$, for

$$\overline{V}_n \equiv \overset{0}{V}_n + \sum_{m=1}^{M_{(n)}} \left(\widehat{V}_{nm} + C_{nm}P_{nm}\right), \tag{10}$$

where

$$\widehat{V}_{nm} \equiv -C_{nm}\left(\overset{0}{P}_n - \overset{0}{P}_m\right), \tag{11}$$

and $\overset{0}{V}_n$, $\overset{0}{P}_n$ and $\overset{0}{P}_m$ are reference values given at the same time (e.g. at $t = 0$).

If we substitute (3), (8)–(11) into (7) we obtain

$$\begin{aligned}\overline{V}_n \frac{\mathrm{d}c^l_n}{\mathrm{d}t} = {} & \sum_{i=1}^{I_{(n)}} Z_{in}P_{in}c^l_{n(n)} - c^l_n\left[\sum_{j=1}^{J_{(n)}} Z_{nj}P_{nj} + \sum_{m=1}^{M_{(n)}} C_{mn}\frac{\mathrm{d}P_{mn}}{\mathrm{d}t}\right] \\ & + \sum_{k=1}^{K_{(n)}} D^l_{kn}\left(c^l_{k(n)} - c^l_n\right) + R^l_n.\end{aligned} \tag{12}$$

Then, by multiplying (5) by c^l_n, and subtracting from (12), we obtain

$$\overline{V}_n \frac{\mathrm{d}c^l_n}{\mathrm{d}t} = \sum_{i=1}^{I_{(n)}} Z_{in}\left(c^l_{n(n)} - c^l_n\right)P_{in} + \sum_{k=1}^{K_{(n)}} D^l_{kn}\left(c^l_{k(n)} - c^l_n\right) - c^l_n Q_{(n)} + R^l_n. \tag{13}$$

Henry's law states that the concentration of a dissolved gas (e.g. CO_2) in a fluid is related to its solubility, α, by

$$c^1_n = \alpha\pi^1_n, \tag{14}$$

where α (constant for all cells) is in mol/l/mm Hg and π^1_n is partial pressure of the gas in cell n. In writing (14), we have overlooked the difference between the volume of a cell and the volume of fluid in it, assuming that the volume of (solid) tissue in the cell is negligible.

Thus, in view of (14), the mass balance equation (13) for the dissolved gas becomes

$$\overline{V}_n \frac{d\pi_n^1}{dt} = \sum_{i=1}^{I_{(n)}} Z_{in}\pi_{in}^1 P_{in} + \sum_{k=1}^{K_{(n)}} D_{kn}^1\left(\pi_{k(n)}^1 - \pi_n^1\right) - \pi_n^1 Q_{(n)} + \frac{R_n^1}{\alpha}, \tag{15}$$

where $\pi_{in}^1 = \pi_i^1 - \pi_n^1$. Note that (15) does not include any efflux terms.

2.2.1. CO_2 *transport.* In view of the transport processes depicted in Fig. 2 and (15), we write the explicit forms of the mass balance equations for dissolved CO_2 in the C, F and B compartments.

Capillary–choroid plexus

$$\text{C:} \qquad \overline{V}_C \frac{d\pi_C^1}{dt} = Z_{AC}\pi_{AC}^1 P_{AC} + D_{BC}^1 \pi_{BC}^1 + D_{FC}^1 \pi_{FC}^1 + \frac{R_C^1}{\alpha}, \tag{16.1}$$

where

$$\overline{V}_C = \overset{0}{V}_C + \widehat{V}_{CF} + C_{CF}P_{CF}. \tag{16.2}$$

CSF

$$\text{F:} \qquad \overline{V}_F \frac{d\pi_F^1}{dt} = \left(Z_{CF}P_{CF} + D_{FC}^1\right)\pi_{CF}^1 + D_{BF}^1 \pi_{BF}^1 + \frac{R_F^1}{\alpha}, \tag{17.1}$$

where

$$\overline{V}_F = \overset{0}{V}_F + \widehat{V}_{FC} + \widehat{V}_{FB} + \widehat{V}_{FS} + C_{CF}P_{CF} + C_{FB}P_{FB} + C_{FS}P_{FS}. \tag{17.2}$$

Brain tissue

In compartment B there are two sources of carbon dioxide production. One is related to hydration–dehydration reaction (R_B^1), the second is CO_2 production in the cells through metabolism. Following Greenberg *et al.* [1], we refer to the assumption that metabolic production rate has two forms: direct production of molecular CO_2 with fraction f' and production of HCO_3^- with fraction $(1 - f')$. Thus balance equation for CO_2 in compartment B has a form:

$$\text{B:} \qquad \begin{aligned} \overline{V}_B \frac{d\pi_B^1}{dt} &= \left(Z_{CB}P_{CB} + D_{BC}^1\right)\pi_{CB}^1 \\ &\quad + \left(Z_{FB}P_{FB} + D_{BF}^1\right)\pi_{FB}^1 + \frac{R_F^1}{\alpha} + \overline{V}_B \frac{Mf'}{\alpha}, \end{aligned} \tag{18.1}$$

where M is the metabolic rate for total CO_2 and

$$\overline{V}_B = \overset{0}{V}_B + \widehat{V}_{BV} + \widehat{V}_{BF} + C_{BV}P_{BV} + C_{FB}P_{FB}. \tag{18.2}$$

With (15) as a typical balance equation for gas such as CO_2 in a compartment, expressed in terms of the partial gas pressure π_n^1, we may write seven balance equations for the seven compartments. Compartment A serves as a compartment with known fluid pressure and partial gas pressure that represent boundary conditions. This leaves only six compartments and six CO_2 balance equations. By examining Fig. 2, we note that the three compartments, C, F and B, contain no influx from the V, S and J compartments. Hence, in view of (15) which disregards the efflux terms, we may write a subsystem of three balance equations for the C, F and B cells in terms of the variables π_C^1, π_F^1 and π_B^1. In order to decouple this subset of transport equations from those for the V, S and J compartments, we had to introduce one more simplifying assumption. This assumption states that the advective CO_2 fluxes between the adjacent compartments from A to C, from C to V, and from B to V, are much larger than the diffusion fluxes between the same compartments. In each case, we may express this assumption by a compartmental Peclet number, expressed in the form

$$\mathrm{Pe}_c = \frac{Z_{\mathrm{in}} P_{\mathrm{in}}}{D_{\mathrm{in}}}. \tag{19}$$

Hence, when $\mathrm{Pe}_c \gg 1$, the advective flux is dominant, while $\mathrm{Pe}_c < 1$ means the domination of the diffusive flux. Otherwise, we have to include both the advective and diffusive fluxes.

Note that in order to evaluate the pressure fall, say between compartments i and j (i.e. P_{ij}), we still need to refer to the entire compartmental setup.

2.2.2. HCO_3^- transport. Our next objective is to write the balance equation for HCO_3^- for the C, F and B compartments. Here we have to take into account the ionic nature of this component. In addition to diffusion across the boundary between adjacent cells, as driven by a concentration difference, another diffusive flux is produced by the difference in electric potential across the boundary. These differences in electrical potential result from the behavior of boundaries as semi-pervious membranes which prevent certain ions from passing through them [1]. Because of the electrical charges and because we deal with the diffusive flux of charged particles (i.e. the HCO_3^- ion) the membrane itself becomes charged and affects the diffusive flux through it.

Nernst's equation describes the *equilibrium* potential created by the ion distributions across the membrane.

The diffusion of an ion through a charged membrane as governed by the electrochemical potential was formulated by Harris [8].

Typical measured values of the electrical potential across membranes for bicarbonate and hydrogen ions [9, 10] do not agree with values as calculated by the Nernst equation. This leads to the conclusion that the Nernst equation does not describe the equilibrium in electro-chemical potentials across a membrane boundary in the cerebral fluids, as produced by the concentrations of HCO_3^- and H^+ ions on both sides of such boundary. Greenberg [1] addresses this issue and suggests an additional diffusive term, controlled by a coefficient of diffusion D''.

Next, we follow Greenberg's [1] development, when applying the component balance equation (13) to HCO_3^- in the C, F and B compartments.

Capillary–choroid plexus

$$\text{C:}\quad \overline{V}_C\frac{dc_C^2}{dt} = Z_{AC}\left(c_A^2 - c_C^2\right)P_{AC} + D_{BC}^2\left(c_B^2 - \gamma_{BC}^2 c_C^2\right) + D_{FC}^2\left(c_F^2 - \gamma_{FC}^2 c_C^2\right) + R_C^2, \tag{20.1}$$

where

$$\left.\begin{aligned} D_{BC}^2 &= D_{BC}'^2 + D_{BC}''^2 \\ \gamma_{BC}^2 &= \frac{D_{BC}'^2}{D_{BC}^2}\cdot\exp\left(-\frac{fZ}{RT}E_m\right)\end{aligned}\right\}, \tag{20.2}$$

$$\left.\begin{aligned} D_{FC}^2 &= D_{FC}'^2 + D_{FC}''^2 \\ \gamma_{FC}^2 &= \frac{D_{FC}'^2}{D_{FC}^2}\cdot\exp\left(-\frac{fZ}{RT}E_m\right)\end{aligned}\right\}. \tag{20.3}$$

In these equations f is Faraday constant, Z is the valence of ion, R is gas constant, T is absolute temperature and E_m is the maximum equilibrium potential according to the Nernst equation

$$E_m = 61.5\log\frac{c'}{c''}, \tag{21}$$

where c' and c'' are concentrations on both sides of the membrane.

CSF

$$\text{F:}\quad \overline{V}_F\frac{dc_F^2}{dt} = Z_{CF}\left(c_C^2 - c_F^2\right)P_{CF} + D_{FC}^2\left(\gamma_{FC}^2 c_C^2 - c_F^2\right) + D_{BF}^2\left(c_B^2 - \gamma_{BF}^2 c_F^2\right) + R_F^2. \tag{22}$$

Here D_{FC}^2, γ_{FC}^2, D_{BF}^2 and γ_{BF}^2 are similar in their expression in (20.2) and (20.3).

Brain tissue

$$\text{B:}\quad \overline{V}_B\frac{dc_B^2}{dt} = Z_{CB}\left(c_C^2 - c_B^2\right)P_{CB} + Z_{FB}\left(c_F^2 - c_B^2\right)P_{FB} + D_{BC}^2\left(\gamma_{BC}^2 c_C^2 - c_B^2\right) + D_{BF}^1\left(\gamma_{BF}^2 c_F^2 - c_B^2\right) + R_B^2 + (1 - f')\overline{V}_B M. \tag{23}$$

From (6), it follows that

$$R_n^1 = -R_n^2 = -R_n^3, \qquad n = \text{B, C, F.} \tag{24}$$

Note that (24) constitutes two equations for each compartment. The concentration of water is assumed constant so that it has no rate of production.

2.2.3. H^+ *transport.* In the case of the hydrogen ion, we realize that a considerable quantity of the formed H^+ becomes bound to various buffers (to hemoglobin in the blood). The bound portion of the total amount does not contribute to changes in pH which is a measure of the (non-bound) concentration of H^+ in the fluid. We define a ***buffer capacity***, β, of a homogeneous medium by the rise in total hydrogen ion concentration, c^{3t}, per unit rise in pH, i.e.

$$\beta = \frac{\mathrm{d}c^{3t}}{\mathrm{d}\,\mathrm{pH}}. \tag{25}$$

The definition of $\mathrm{pH}(= -\log c^3)$, together with (25) yields

$$\frac{\mathrm{d}c^{3t}}{\mathrm{d}t} = -\frac{\beta}{(\ln 10)c^3}\frac{\mathrm{d}c^3}{\mathrm{d}t}. \tag{26}$$

The integration of (25) for compartments n and i (assuming β to be constant within the range encountered in the compartments) yields

$$c_i^{3t} - c_n^{3t} = \beta(\mathrm{pH}_i - \mathrm{pH}_n) - (B_n - B_i), \tag{27}$$

where B_n and B_i are integration constants associated with compartments n and i, respectively.

The discussion presented above on the diffusion of the bicarbonate ion across boundaries between adjacent compartments is also applicable to the hydrogen ions.

In view of (12), (26) and (27), we write the mass balance equations for the H^+ ion in compartments C, F and B.

Capillary–choroid plexus

C:
$$\overline{V}_{\mathrm{C}}\frac{\mathrm{d}c_{\mathrm{C}}^3}{\mathrm{d}t} = -\frac{\ln 10}{\beta_{\mathrm{C}}}c_{\mathrm{C}}^3\Big[Z_{\mathrm{AC}}(\beta\mathrm{pH}_{\mathrm{AC}} - B_{\mathrm{CA}})P_{\mathrm{AC}} + D_{\mathrm{BC}}^3\left(c_{\mathrm{B}}^3 - \delta_{\mathrm{BC}}^3 c_{\mathrm{C}}^3\right) + D_{\mathrm{FC}}^3\left(c_{\mathrm{F}}^3 - \delta_{\mathrm{FC}}^3 c_{\mathrm{C}}^3\right) + R_{\mathrm{C}}^3\Big], \tag{28.1}$$

where

$$\left.\begin{aligned} D_{\mathrm{BC}}^3 &= D_{\mathrm{BC}}'^3 \\ \delta_{\mathrm{BC}}^3 &= \frac{D_{\mathrm{BC}}'^3 \exp\left(\frac{fZ}{RT}E_{\mathrm{m}}\right) + D_{\mathrm{BC}}''^3}{D_{\mathrm{BC}}^3} \end{aligned}\right\}, \tag{28.2}$$

$$\left.\begin{aligned} D_{\mathrm{FC}}^3 &= D_{\mathrm{FC}}'^3 \\ \delta_{\mathrm{FC}}^3 &= \frac{D_{\mathrm{FC}}'^3 \exp\left(\frac{fZ}{RT}E_{\mathrm{m}}\right) + D_{\mathrm{FC}}''^3}{D_{\mathrm{FC}}^3} \end{aligned}\right\}. \tag{28.3}$$

Here $\mathrm{pH}_{ij} \equiv \mathrm{pH}_i - \mathrm{pH}_j$ and $B_{ij} \equiv B_i - B_j$.

CSF

$$\text{F:}\quad \overline{V}_F\frac{dc_F^3}{dt} = -\frac{\ln 10}{\beta_F}c_F^3\Big[Z_{CF}(\beta pH_{CF} - B_{CF})P_{CF} + D_{FC}^3\Big(\delta_{FC}^3 c_C^3 - c_F^3\Big) + D_{BF}^3\Big(c_B^3 - \delta_{BF}^3 c_F^3\Big) + R_F^3\Big]. \tag{29}$$

Here D_{FC}^3, δ_{FC}^3, D_{BF}^3 and δ_{BF}^3 have expressions similar to those given in (28.2) and (28.3).

Brain tissue

$$\text{B:}\quad \overline{V}_B\frac{dc_B^3}{dt} = -\frac{\ln 10}{\beta_B}c_B^3\Big[Z_{CB}(\beta pH_{CB} - B_{CB})P_{CB} + Z_{FB}(\beta pH_{FB} - B_{FB})P_{FB} + D_{BC}^3\Big(\delta_{BC}^3 c_C^3 - c_B^3\Big) + D_{BF}^3\Big(\delta_{BF}^3 c_F^3 - c_B^3\Big) + R_B^3 + (1-f')M\overline{V}_B\Big]. \tag{30}$$

The presence of the enzyme carbonic anhydrase in the red blood cells makes the hydration/dehydration practically instantaneous. Consequently reaction (6) is always one of equilibrium, described by the reaction constant k.

On the other hand, in compartment F the absence of carbonic anhydrase in the cerebral extracellular fluid means that reaction is not one of equilibrium. Instead, it has a finite constant rate. We assume a first-order reaction in which the rate is proportional to the concentration. Under conditions of non-equilibrium, the rate of production of CO_2 equals the difference between the reverse and forward reaction rates. Therefore, in view of (6) and (14), we write for the F compartment

$$R_F^1 = \overline{V}_F\Big(k_R c_F^3 c_F^2 - k_F \alpha\pi_F^1\Big). \tag{31}$$

In compartments C and B, where the reaction is in equilibrium, we write

$$k = \frac{c^3 c^2}{c^1}. \tag{32}$$

Concentration of water (H_2O) is assumed constant; hence, it is incorporated in the reaction constant k. By virtue of (14) and (32) we conclude that $c^3 = c^3(\alpha\pi^1, c^2)$. Therefore, we can replace (32) for compartments C and B, by the relation

$$\frac{dc^3}{dt} = -\frac{c^3}{c^2}\frac{dc^2}{dt} + \frac{\alpha k}{c^2}\frac{d\pi^1}{dt}. \tag{33}$$

2.3. Numerical solution

At this stage we have a model consisting of 24 unknown variables (six P_j pressures associated with compartments $j = B, C, F, V, S, J$; nine c_n^l concentrations and nine R_n^l, sink-source terms, $l = 1, 2, 3$ for CO_2, HCO_3^- and H^+, respectively, associated with compartments $n = B, C, F$) for which we have 24 coupled equations: six balance

equations (5) for blood flow, one for each compartment; nine component mass balance equations (16.1), (17.1), (18.1), (20.1), (22), (23), (28.1), (29) and (30), one for each component in each compartment; two relations (33) for compartments C and B, expressing the reaction kinetics; equation (31) for compartment F, and six reaction balance equations (24), for compartments C, F and B.

Taking into account (24) we can rewrite the mass balance equations (16.1), (18.1), (19.1), (22), (27.1), (29) in compartments B and C, in the form

$$\overline{V}_n \frac{\mathrm{d}\pi_n^1}{\mathrm{d}t} = \varphi_n^1 + \frac{R_n^1}{\alpha}, \qquad n \equiv \mathrm{B}, \mathrm{C}, \tag{34.1}$$

$$\overline{V}_n \frac{\mathrm{d}c_n^2}{\mathrm{d}t} = \varphi_n^2 - R_n^1, \tag{34.2}$$

$$-\frac{\beta_n^*}{c_n^3}\overline{V}_n \frac{\mathrm{d}c_n^3}{\mathrm{d}t} = \varphi_n^3 - R_n^1, \qquad \beta_n^* = \frac{\beta_n}{\ln 10}. \tag{34.3}$$

where φ_n^l denotes the right-hand side of (16.1), (18.1), (19.1), (22), (27.1) and (29), excluding the reaction terms R_n^l $(l = 1, 2, 3)$.

After substitution of (34) into (33) we obtain

$$R_n^1 = \sum_{l=1}^{3} a_n^l \varphi_n^l, \qquad n \equiv \mathrm{B}, \mathrm{C}, \tag{35.1}$$

where

$$a_n^1 \equiv -\frac{\alpha k}{c_n^2 \Delta_n}, \quad a_n^2 \equiv \frac{c_n^3}{c_n^2 \Delta_n}, \quad a_n^3 \equiv -\frac{c_n^3}{\beta_n^* \Delta_n}, \tag{35.2}$$

and

$$\Delta \equiv \frac{k}{c_n^2} + \frac{c_n^3}{c_n^2} - \frac{c_n^3}{\beta_n^*}. \tag{35.3}$$

Finally equations (34) can be rewritten as

$$\overline{V}_n \frac{\mathrm{d}\pi_n^1}{\mathrm{d}t} = \left(1 + \frac{a_n^1}{\alpha}\right)\varphi_n^1 + \frac{a_n^2 \varphi_n^2}{\alpha} + \frac{a_n^3 \varphi_n^3}{\alpha}, \qquad n \equiv \mathrm{B}, \mathrm{C}, \tag{36.1}$$

$$\overline{V}_n \frac{\mathrm{d}c_n^2}{\mathrm{d}t} = -a_n^1 \varphi_n^1 + (1 - a_n^2)\varphi_n^2 - a_n^3 \varphi_n^3, \tag{36.2}$$

$$\overline{V}_n \frac{\mathrm{d}c_n^3}{\mathrm{d}t} = -\frac{c_n^3}{\beta_n^*}\left[-a_n^1 \varphi_n^1 - a_n^2 \varphi_n^2 + (1 - a_n^3)\varphi_n^3\right]. \tag{36.3}$$

In compartment F, using (23) and (30) we transform (17.1), (21) and (28) into

$$\overline{V}_F \frac{d\pi_F^1}{dt} = \varphi_F^1 + \frac{\overline{V}_F}{\alpha}\left(k_R c_F^3 c_H^2 - k_F \alpha \pi_F^1\right), \tag{36.4}$$

$$\overline{V}_F \frac{dc_F^2}{dt} = \varphi_F^2 - \frac{\overline{V}_F}{\alpha}\left(k_R c_F^3 c_F^2 - k_F \alpha \pi_F^1\right), \tag{36.5}$$

$$\overline{V}_F \frac{dc_F^3}{dt} = -\frac{c_F^3}{\beta_F^*}\left[\varphi_F^2 - \frac{\overline{V}_F}{\alpha}\left(k_R c_F^3 c_F^2 - k_F \alpha \pi_F^1\right)\right]. \tag{36.6}$$

Thus for nine unknowns π_n^1, c_n^2, c_n^3 ($n = B, C, F$) we have nine equations (36).

To solve (5) for the six compartmental hydrodynamic pressures P_n, together with (36) for three CO_2 partial pressure π_n^1, three HCO_3^- concentrations c_n^2 and three H^+ concentrations c_n^3, we need initial values. These are given in Table 1.

In compartment A we prescribe the arterial pressure and flow [3]

$$P_A = P_A^* + P_A' \sin 2\pi\omega t, \tag{37}$$

$$Q_A = Q_A^* + Q_A' \sin 2\pi\omega t, \tag{38}$$

where P_A^* and P_A' denote the average arterial pressure and its amplitude, respectively, Q_A^* and Q_A' denote the average arterial flow and its amplitude, respectively, ω denotes the cardiac frequency. The concentration of the components in the artery (π_A^1, c_A^2, c_A^3) are prescribed in time.

The system of nonlinear ordinary differential equations (5) and (36) were solved by the Runge–Kutta method of the fourth order with adaptive stepsize control.

3. RESULTS

3.1. Blood flow control

In writing the balance equation (5), it is usually assumed that the conductances, Z, are independent of time. However, in reality, the values of Z vary continuously in response to certain changes that occur in the cerebrovascular system. In what follows the brain cells are continuously metabolizing, consuming oxygen and producing CO_2. The changes in the CO_2 production are probably the dominant factor in cerebral blood flow control.

We use a relation [11] between CO_2 tension in the CSF (π_F^1) and in the arteries (π_A^1).

$$\pi_F^1 = 8.6 + 0.942\pi_A^1. \tag{39}$$

Table 1.
Parameters used in the model simulations [1–5]

Parameter	'Nominal' $[(\cdot)_{nom}]$ value	Range
Initial values		
P_A, mmHg	100.0	
P_B, mmHg	8.7	
P_C, mmHg	30.0	
P_F, mmHg	9.4	
P_V, mmHg	8.5	
P_S, mmHg	7.5	
P_J, mmHg	1.3	
π_B^1, mmHg	49.5	
π_C^1, mmHg	47.9	
π_F^1, mmHg	48.6	
c_B^2, mmol/l	15.3	
c_C^2, mmol/l	27.6	
c_F^2, mmol/l	23.9	
pH_B	7.10	
pH_C	7.37	
pH_F	7.30	
Arterial variables		
P_A^*, mmHg	110.0	
P_A', mmHg	20.0	
Q_A', ml/min	120.0	
π_A^1, mmHg	50.0	
c_A^2, mmol/l	30.9	
pH_A	7.4	
ω, Hz	1.0	
Physical and chemical parameters		
$\overline{V}_B$, ml	996	$(0.90-1.03)\cdot(\overline{V}_B)_{nom}$
$\overline{V}_C$, ml	30	$(0.80-1.20)\cdot(\overline{V}_C)_{nom}$
$\overline{V}_F$, ml	150	$(0.10-0.15)\cdot(\overline{V}_F)_{nom}$
α, mol/(l · mmHg)	10.31×10^{-4}	
k, mol/l	7.94×10^{-7}	
k_F, 1/s	0.131	$(10^{-2}-10^{2})\cdot(k_F)_{nom}$
k_R, 1/(mol · s)	1.65×10^{5}	$(10^{-2}-10^{2})\cdot(k_R)_{nom}$
M, mmol/(l · min)	2.17	$(0.75-1.15)\cdot(M)_{nom}$
f'	0.9	$(0.55-1.1)\cdot(f')_{nom}$

Table 1.
(Continued)

Parameter	'Nominal' $[(\cdot)_{nom}]$ value	Range
Buffering parameters		
β_B, mmol/(l · pHunit)	−20	$(0.75-1.40)\cdot(\beta_B)_{nom}$
β_C, mmol/(l · pHunit)	−12	$(0.90-1.15)\cdot(\beta_C)_{nom}$
β_F, mmol/(l · pHunit)	−18.5	$(0.65-1.30)\cdot(\beta_F)_{nom}$
B_{CA}, mmol/l	2.07	$(0.55-1.05)\cdot(B_{CA})_{nom}$
B_{FC}, mmol/l	2.07	$(0.55-1.05)\cdot(B_{FC})_{nom}$
B_{BC}, mmol/l	2.07	$(0.55-1.05)\cdot(B_{BC})_{nom}$
B_{BF}, mmol/l	2.07	$(0.55-1.05)\cdot(B_{BF})_{nom}$
Conductances and compliances		
Z_{AC}, ml/(mmHg · min)	10.7	
Z_{BC}, ml/(mmHg · min)	0.000075	
Z_{BF}, ml/(mmHg · min)	0.075	
Z_{BV}, ml/(mmHg · min)	0.3	
Z_{CF}, ml/(mmHg · min)	0.015	
Z_{FS}, ml/(mmHg · min)	0.13	
Z_{SV}, ml/(mmHg · min)	76.9	
Z_{JS}, ml/(mmHg · min)	125.0	
Z_{CV}, ml/(mmHg · min)	35.7	
C_{AB}, ml/mmHg	0.0012	
C_{CF}, ml/mmHg	0.0360	
C_{BV}, ml/mmHg	0.375	
C_{FS}, ml/mmHg	0.0490	
C_{BF}, ml/mmHg	0.2090	
Diffusion parameters		
$\gamma^2_{BC}(=\gamma^2_{BF}=\gamma^2_{BC})$	0.074	$(0.65-6.75)\cdot(\gamma^2_{BC})_{nom}$
$\delta^3_{BC}(=\delta^3_{BF}=\delta^3_{BC})$	0.93	$(0.90-1.10)\cdot(\delta^3_{BC})_{nom}$
D^1_{BC}, l/min	37.5	$(10^{-1}-10)\cdot(D^1_{BC})_{nom}$
D^1_{FC}, l/min	9.79	$(10^{-1}-10)\cdot(D^1_{FC})_{nom}$
D^1_{BF}, l/min	8.52	$(10^{-1}-10)\cdot(D^1_{BF})_{nom}$
D^2_{BC}, l/min	0.00830	$(10^{-1}-5)\cdot(D^2_{BC})_{nom}$
D^2_{FC}, l/min	0.00798	$(10^{-1}-2)\cdot(D^2_{FC})_{nom}$
D^2_{BF}, l/min	0.00387	$(10^{-1}-5)\cdot(D^2_{BF})_{nom}$
D^3_{BC}, l/min	0.03010	$(10^{-1}-10)\cdot(D^3_{BC})_{nom}$
D^3_{FC}, l/min	0.00471	$(10^{-1}-10)\cdot(D^3_{FC})_{nom}$
D^3_{2F}, l/min	0.04450	$(10^{-1}-10)\cdot(D^3_{3F})_{nom}$

Following Greenberg *et al.* [1], we also use the relation between average arterial to capillary flow ($\bar{q}_{AC}$) and the arterial CO_2 pressure (π_A^1) [12].

$$\bar{q}_{AC} = 20.9 + \frac{92.8}{1 + 10570(\pi_A^1)^{-2.281}}. \tag{40}$$

Note that π_A^1 and $\bar{q}_{AC}$ are expressed in [mmHg] and [ml/(100 g min)], respectively.

An increase in the amount of CO_2 in the arterial blood bathing the brain causes a dilation of blood vessels and an increase in the blood flow which carries away CO_2 and re-establishes normal conditions.

By combining (39) and (40) we find the relation between $\bar{q}_{AC}$ and π_F^1,

$$\bar{q}_{AC} = 20.9 + \frac{92.8}{1 + 10570\left(\frac{\pi_F^1 - 8.6}{0.942}\right)^{-2.281}}. \tag{41}$$

Following (5) when applied to compartment A,

$$C_{AB}\frac{dP_{AB}}{dt} + q_{AC} = Q_A, \tag{42}$$

where we choose compliance $C_{AB} = 0.0012$ ml/mmHg [5]. Integration of (42) over the interval of one time cycle $[t_0,\ t_1 = t_0 + 1/\omega]$ and bearing in mind the cyclic behavior of pressure, we obtain

$$\bar{q}_{AC} = Q_A^*. \tag{43}$$

Since flow between compartments A and C is proportional to the conductance Z_{AC}, we postulate that

$$Z_{AC} = Z_{AC}^0 \frac{Q_A^*}{Q_A^{*0}}, \tag{44}$$

where Z_{AC}^0 denotes the conductance at a known reference flow Q_A^{*0}. For example, when solving the inverse problem for the flow equations (5), it was found that for $Q_A^{*0} = 50$ ml/(100 g min) the associate conductance values is $Z_{AC}^0 = 10.7$ ml/(mmHg min) [5]. Thus by virtue of (38), (41) and (44) the flow and transport problems are coupled.

In the set (5) and (36), we encounter various coefficients, or parameters. One group consists of coefficients such as $k_F, k_R, \alpha, \ldots$ that are universal and assumed known. They are independent of the particular model employed here. The second group consists of the conductances Z_{ni}, compliances C_{ni} and boundary diffusivities D_{ni}^l. The determination of the coefficients Z_{ni}, and C_{ni} was described in an earlier paper [3] and will be considered here as already known.

In the following section, we shall consider the estimation of the various boundary diffusivities of the model.

3.2. Estimating boundary diffusivity coefficients

In order to estimate nine diffusion coefficients we use (36) at quasi-steady-state conditions.

As the CO_2 mass (as well as that of HCO_3^- and H^+) within each compartment varies, we may identify points in time, say t_1 and t_2 ($> t_1$), at which this mass is the same. This means that over the time interval between t_1 and t_2 (regardless of the sequence of changes in between these instances), the total mass of CO_2 in the compartment has not changed. Hence

$$\int_{t_1}^{t_2} \overline{V} \frac{\partial c}{\partial t} \, dt = 0, \qquad \overline{V}c\big|_{t_1} = \overline{V}c\big|_{t_2}. \tag{45}$$

Thus by integrating (36) over a period of time beginning and ending with the same component mass, we obtain a system of linear algebraic equations

$$\mathbf{AD} = \mathbf{B}, \tag{46}$$

where $\mathbf{D} = [D^1_{BC}, D^1_{FC}, D^1_{BF}, D^2_{BC}, D^2_{FC}, D^2_{BF}, D^3_{BC}, D^3_{FC}, D^3_{BF}]$ denote the unknown vector. Matrix $\mathbf{A}$ and vector $\mathbf{B}$ relate to average concentrations, quasi steady-state values of pressures and various model parameters. However, we note that $\mathbf{A}$ is singular. Hence, special considerations are needed and therefore a set of techniques, known as singular value decomposition, were implemented [13]. In order to reduce the number of nonzero elements in $\mathbf{A}$, we considered the case when chemical equilibrium between CO_2, HCO_3^- and H^+ components also exists in compartment F. Thus (35) and (36.1)–(36.3) for $n = F$ were used instead of (36.4)–(36.6). Numerical experiments show that in this case the obtained solution is more stable in relation to the input of small deviations from the initial data. Solution of the inverse problem needs numerical values of components concentration and parameters, which are accepted as known. Most of these were taken as a data base from Greenberg *et al.* [1] and are presented in Table 1. The estimated diffusions were found to be rather sensitive to the input concentrations data. Diffusivities of HCO_3^- and H^+ were more sensitive than that of CO_2. The following subset were introduced in (46)

$$\pi^1_A = 40.0 \text{ mmHg}, \quad \pi^1_B = 49.5 \text{ mmHg}, \quad \pi^1_C = 47.9 \text{ mmHg}, \quad \pi^1_F = 48.6 \text{ mmHg},$$
$$c^2_A = 24.7 \text{ mmol/l}, \quad c^2_B = 15.3 \text{ mmol/l}, \quad c^2_C = 27.6 \text{ mmol/l}, \quad c^2_F = 23.9 \text{ mmol/l},$$
$$pH_A = 7.40, \quad pH_B = 7.10, \quad pH_C = 7.37, \quad pH_F = 7.27.$$

and produced the following boundary diffusivities, D^l_{kn} (l/min):

CO_2:	$D^1_{BC} = 37.50$,	$D^1_{FC} = 9.79$,	$D^1_{BF} = 8.52$.
HCO_3^-:	$D^2_{BC} = 0.00830$,	$D^2_{FC} = 0.00798$,	$D^2_{BF} = 0.00387$,
H^+:	$D^3_{BC} = 0.03010$,	$D^3_{FC} = 0.00471$,	$D^3_{BF} = 0.04450$.

In order to check the validity of the obtained D_{kn}^{l} diffusivities, we use their values for the solution of (36) for a long time period. This will yield the quasi-steady-state values of the variables. The obtained values were

$$\pi_B^1 = 49.6 \text{ mmHg}, \quad \pi_C^1 = 47.9 \text{ mmHg}, \quad \pi_F^1 = 48.6 \text{ mmHg},$$
$$c_B^2 = 14.7 \text{ mmol/l}, \quad c_C^2 = 27.5 \text{ mmol/l}, \quad c_F^2 = 20.8 \text{ mmol/l},$$
$$\text{pH}_B = 7.08, \quad \text{pH}_C = 7.37, \quad \text{pH}_F = 7.22.$$

As expected, these were similar to the values of the same variables implemented in the inverse procedure. The maximum deviation (13%) occurs in the HCO_3^- concentration associated with compartment F. For the other variables, the differences are less significant.

3.3. Sensitivity analysis

In order to investigate the effect of the various parameters on model behavior, a sensitivity analysis was performed. Each parameter (independent of all others) was varied within its admissible limits (see Table 1). We examined the influence of these parameters on component concentrations and arterial flow for the case in which arterial CO_2 tension has a step change from 40 to 50 mmHg. Some of the results which showed appreciable changes in the model behavior are presented in Figs 4–9. All comparisons were made relative to a 'nominal' set of parameters listed in column 2 of Table 1. Note that 'decrease' or 'increase' of variables will be referred to as the behavior relative to the simulation based on the 'nominal' set.

The performed sensitivity analysis showed that changes of $\overline{V}_C$, $\overline{V}_F$, α, k, k_L, k_R, f', β, δ and D_{kn}^{3} had very little effect on concentration of components and arterial flow. Other parameters had a different influence in different compartments.

Parameter of CO_2 metabolic rate, M, had a similar influence on CO_2 tension in all compartments. Its increase or decrease constitutes the same trend when considering CO_2 pressure (Figs 4–6). Accordingly, changes of CO_2 concentration in the CSF compartment leads to changes of the mean arterial flow (Fig. 7). This phenomenon is well observed clinically [14].

It was found that the brain tissue volume had a small influence only on the CO_2 pressure. A decrease of $\overline{V}_B$ to 90% of its 'nominal' value induces a decrease of CO_2 partial pressure in all compartments, mainly because of a reduction of the total metabolic CO_2 production.

Among the B_{kn} parameters characterizing the Haladane effect, only B_{CA} had a considerable influence on model behavior. Hence, this effect is mainly pronounced between artery and capillaries. Lowering of B_{CA} results in the rise of CO_2 partial pressure and the fall of HCO_3^- concentration and pH in all compartments (Figs 4–6), and an increase of mean arterial flow (Fig. 7).

The disequilibrium transport coefficient of bicarbonate ion, γ, which represents the active transport induced by electrochemical potential, had an identifiable influence only on changes of HCO_3^- concentration and pH. Its augmentation from 0.074 to

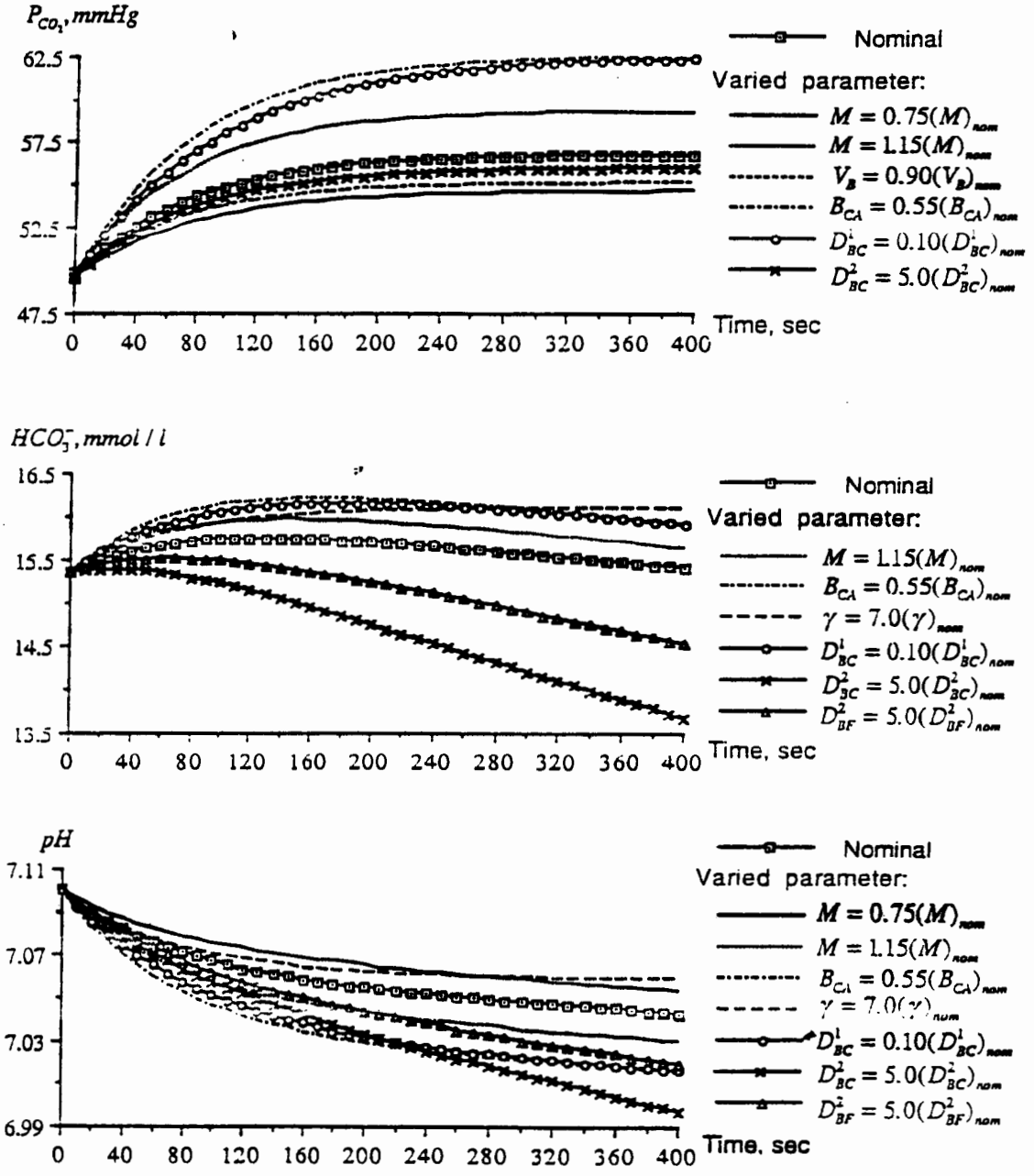

Figure 4. Effect of change in parameters on evolution of components in the brain tissue compartment.

0.5 led to the increase of bicarbonate concentration in the brain tissue and CSF compartment (Figs 4 and 6), and a decrease of HCO_3^- concentration in the capillary and the choroid plexus (Fig. 5). Changes in HCO_3^- concentration through the mechanism of chemical equilibrium reaction induced an increase of the pH in brain tissue and CSF compartments, and a less significant decrease in the capillary compartment.

Numerical simulations show that boundary diffusivities play an important role in transport of chemicals between the compartments. However, their contributions are

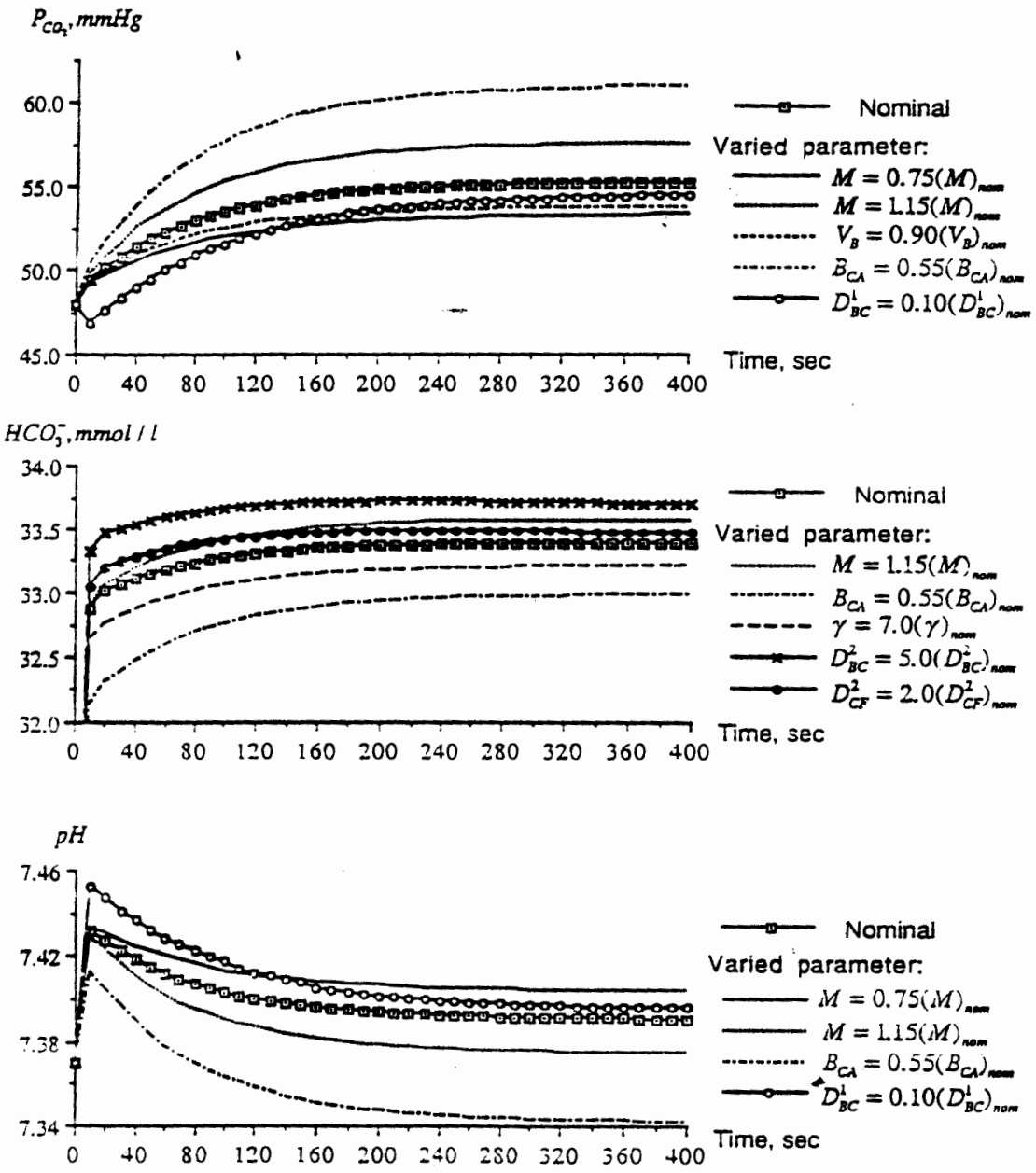

Figure 5. Effect of change in parameters on evolution of components in the capillary compartment.

different. It was found that a 10-fold reduction of any of the coefficients had no significant effect excluding D^1_{BC}. A decrease in D^1_{BC} leads to the growth of the CO_2 gradient between the brain tissue and capillary compartments. At the same time, CO_2 pressure increased in the brain tissue and CSF compartments, and decreased in the capillary compartment. Mean arterial flow also increased (Fig. 7), as well as the concentrations of HCO_3^- and H^+ in the brain tissue compartment (Fig. 4). Changes of the two latter in capillary and CSF are smaller and are demonstrated only for pH in capillary (Fig. 5).

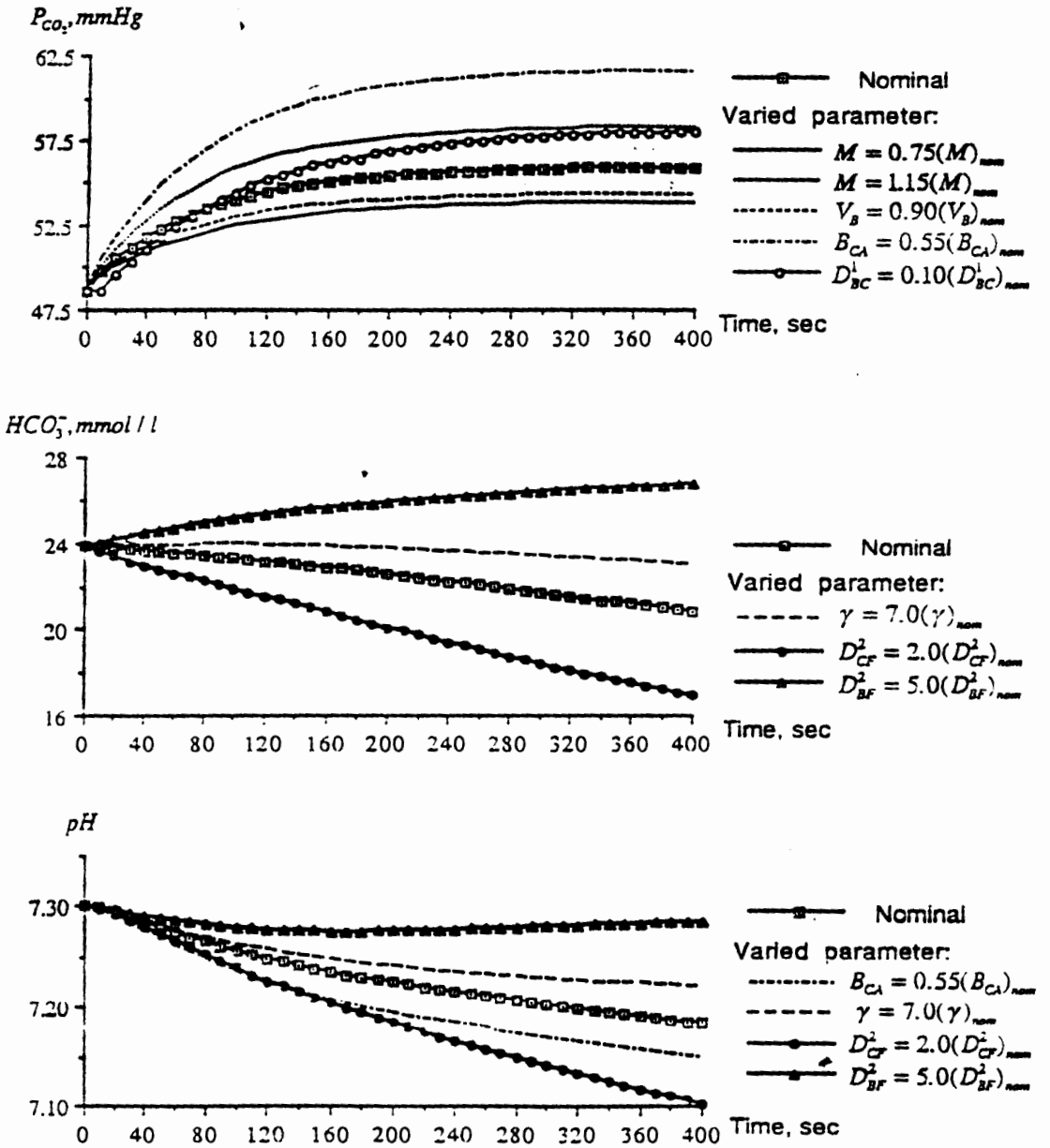

Figure 6. Effect of change in parameters on evolution of components in the CSF compartment.

An increase of boundary diffusivities for CO_2 induced the reduction of CO_2 partial pressure gradient between C, F and B compartments, and did not show any significant influence on the behavior of the hydrocarbonate and hydrogen ions. The same behavior was experienced by the boundary diffusivity coefficients of H^+.

Diffusion coefficients of HCO_3^- almost did not exert any influence on the behavior of CO_2. However, HCO_3^- concentration and pH in different compartments were rather sensitive to changes of this parameter. For example, a 5-fold increase of D^2_{BC} caused a drastic drop of the HCO_3^- concentration and pH in the brain tissue, and a less considerable rise of HCO_3^- in the capillary (Figs 4 and 5). Yet, when increasing coefficient

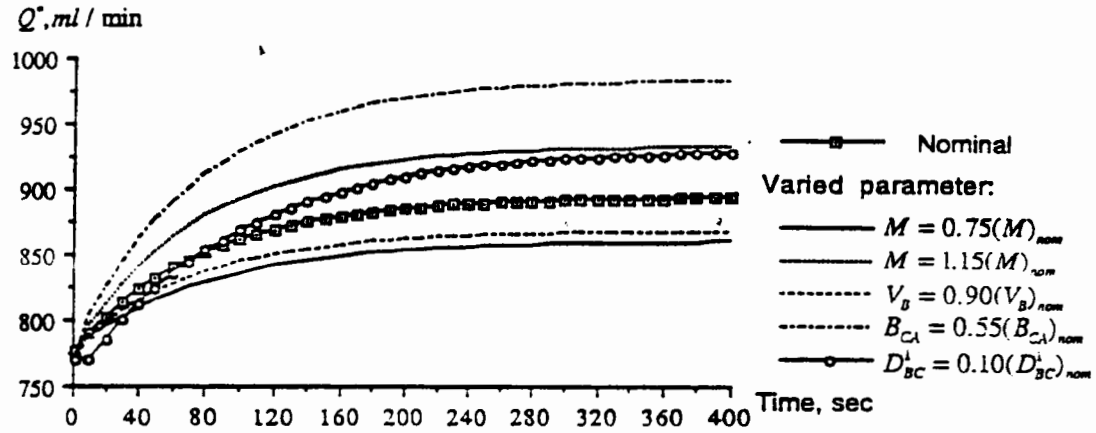

Figure 7. Effect of change in parameters on evolution of mean flow in the artery compartment.

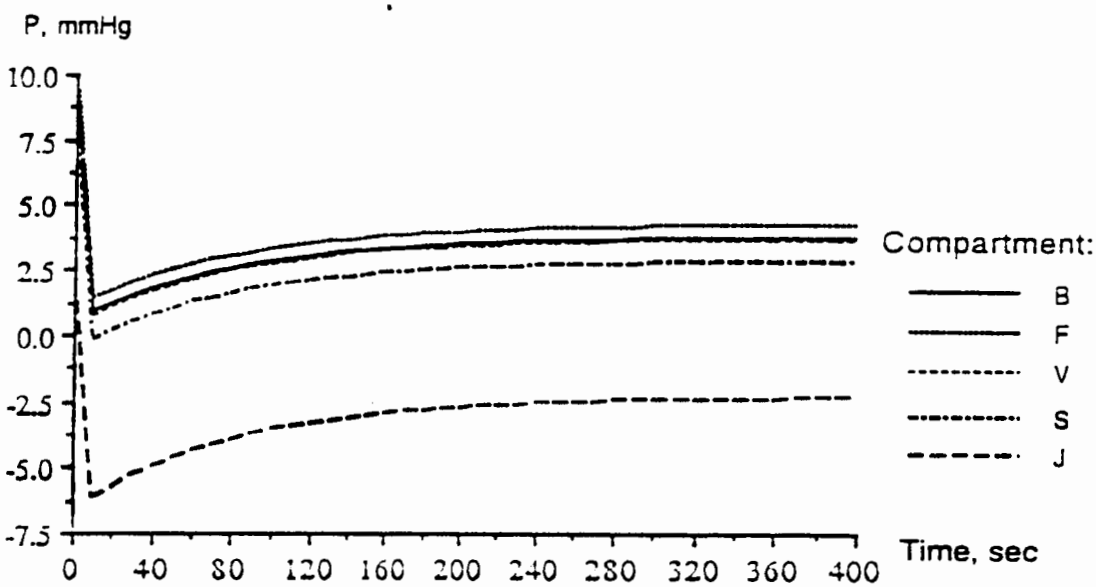

Figure 8. Response of compartment's mean blood pressure due to the decrease of arterial CO_2 partial pressure from 40 to 30 mmHg.

D^2_{FC} only 2-fold, it induced a dramatic decrease of HCO_3^- in the CSF compartment (Fig. 6), without affecting other components.

Parameter D^2_{BF} affected HCO_3^- concentration and pH in compartment B similar to D^2_{BC}, i.e. its augmentation increased the value of the simulated HCO_3^- and pH variables. In compartment F, D^2_{BF} had an opposite effect (Fig. 6).

Thus, we note that model behavior is rather sensitive to changes in boundary diffusivities. This indicates the importance in obtaining a better assessment of their values not only at the quasi-steady-state stage at which the distribution of compartmental concentration is achieved. Hence a more detailed measurement during non-steady state conditions should be used in order to solve the inverse problem.

Figure 8 exemplifies the response of the mean blood pressure due to a decrease in CO_2 partial pressure in the artery (when it drops from 40 to 30 mmHg). Simultane-

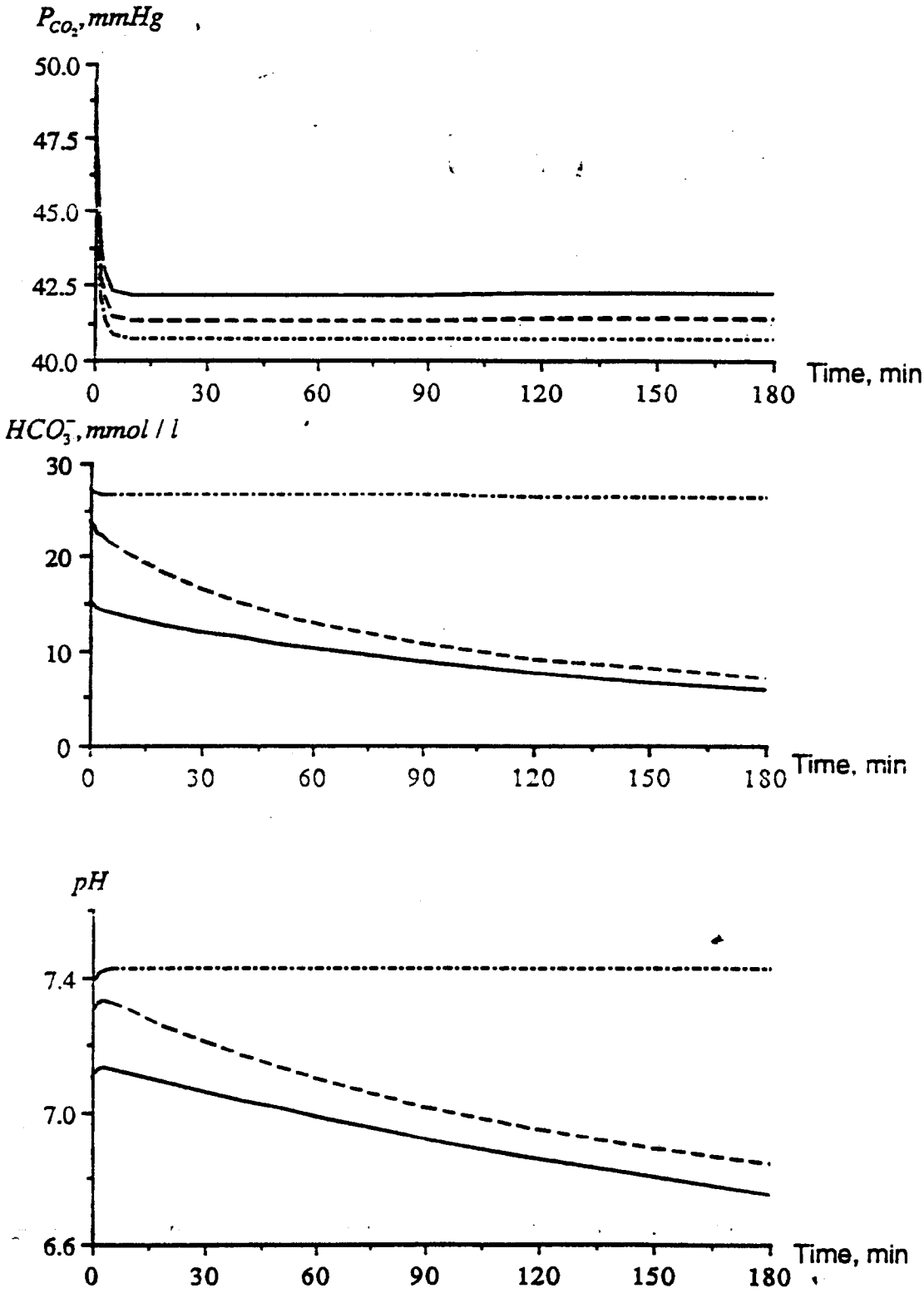

Figure 9. Evolution of the components in the compartments B (——), C (·····) and F (- - -) due to fall of arterial P_{CO_2} from 40 to 30 mmHg.

ously, we had also dropped the arterial pressure from 100 to 90 mmHg. Changes of blood pressure are induced by alterations of arterial mean flow and the conductance Z_{AC} (see equation (43)). We note an abrupt fall of pressure at the first instance reaching an asymptotic value with time, in all compartments except that of the capillary. In the capillary (not shown) the pressure abruptly falls from 30 to 20.6 mmHg and remains at that level with a very slow increase rate. Figure 9 shows the evolution of the components in this case. The CO_2 partial pressure drops at first time instances and then increases very slowly in all compartments. The HCO_3^- concentration in the capillary slightly falls and then remains constant during time. We note that it decreases gradually in the CSF and brain tissue compartments. Accordingly, the pH in the capillary increases slightly and then remains constant. In the CSF and brain tissue compartments, pH decreases with time after an initial rise. This trend of P_{CO_2}, HCO_3^- and pH in the CSF is qualitatively similar to the experiments performed in rabbits during sustained hyperventilation [14].

4. CONCLUSION

A compartmental brain model was developed to describe transport processes of molecular CO_2, HCO_3^- and H^+ between brain tissue (B), capillary–choroid plexus (C) and the CSF (F) compartments. The model consists of mass balance equations (i.e. transport equations) accounting for non-steady advection, diffusion and generation of constituents due to chemical reactions.

Balance equations are expressed in tension values of CO_2, concentration for HCO_3^- and free concentration for H^+.

The fluid is assumed to be of a constant density, hence allowing decoupling between the solutions of fluid and of component balance equations. A separate solution is thus obtained for non-steady flow through the cerebrovascular system model by seven compartments: artery, capillary–choroid plexus, brain tissue, CSF, vein, venous sinus and jugular bulb. This solution describes the evolution of compartmental perfusion pressure subject to conductances expressing the case of leakage through semi-pervious boundaries and compliances expressing compartmental volume rate of change due to boundary displacements [3–5]. The non-steady flow governs the advection term in the model describing the transport of chemical components. This enables the study of pathological situations such as different patterns of initial fluxes that give rise to transient periods of transport, and/or changes in conductances and compliances because of occlusions.

Generation of components in the physiological fluid within a compartment is governed by the stochiometric relation expressing the hydration reaction. Within the capillary–choroid plexus and the CSF compartments, the reaction is considered to be instantaneous, hence in equilibrium. Within the brain tissue compartment, the production of CO_2 is assumed to equal the difference between the reverse and forward reaction rates.

In order to solve for the different components, we need to know various coefficients. Some of them may be found in different citations. However, most of the boundary diffusivities need still to be estimated. Therefore, we present a parameter

estimation method which we implement to assess time averaged boundary diffusivities based on time observations of perfusion pressures, CO_2 tension, HCO_3^- concentration and pH. An assessment of the sensitivity of the transport solution to parameters such as diffusivities, various physical and chemical parameters was also investigated.

Diffusivities, compliances and conductances are assumed as average values in time, i.e. they may change from one constant value to another because of reasons such as illness, aging, etc. We relax this assumption for the conductance, Z_{AC}, controlling flow from the arteries to the capillaries. We introduce an equation of state that relates this conductance to perfusion pressure drop between arteries and capillaries and CO_2 tension in the CSF. Hence, Z_{AC} is changing continuously in response to excitations from the perfusion pressure and CO_2 tension. This short time of response of Z_{AC} describes flow control from arteries to capillaries.

REFERENCES

1. J. H. Greenberg, M. Relvich and A. Noordergraph. A model of cerebral blood flow control in hypercapnia. *Ann. Biomed. Eng.* **6**, 453–491 (1978).
2. Z. Karni, J. Bear, S. Sorek and Z. Pinczewski. Quasi-steady-state compartment model of intracranial fluid dynamics. *Med. Biol. Eng. Comput.* **25**, 167–172 (1987).
3. S. Sorek, J. Bear and Z. Karni. A non-steady compartmental flow model of the cerebrovascular system. *J. Biomechanics* **21**, 695–704 (1988).
4. S. Sorek, J. Bear and Z. Karni. Intracranial compartment pulse wave simulation. *Math. Biosci.* **89**, 149–159 (1988).
5. S. Sorek, J. Bear and Z. Karni. Resistances and compliances of a compartmental model of the cerebrovascular systems. *Ann. Biomed. Eng.* **17**, 1–12 (1989).
6. E. A. Bering, Jr. Choroid plexus and arterial pulsation of cerobrospinal fluid. Demonstration of the choroid plexus as a cerebrospinal fluid pump. *Arch. Neurol. Psych.* 73, 165–172 (1955).
7. H. Davson. *Physiology of the Cerebrospinal Fluid.* Churchill, London (1967).
8. E. S. Harris. *Transport and Accumulation in Biological Systems*, 2nd edn. Academic Press, New York (1960).
9. K. Messeter and B. K. Siesjo. Electrochemical gradients for H^+ and HCO_3^- between blood and CSF during sustained acid–base changes. In: *Ion Homeostasis of the Brain*, B. K. Siesjo and S. C. Sorensen (Eds). Academic Press, New York (1971).
10. S. C. Sorensen. Factors regulating H^+ and HCO_3^- in the brain extracellular fluid. In: *Ion Homeostasis of the Brain*, B. K. Siesjo and S. C. Sorensen (Eds). Academic Press, New York (1971).
11. V. Ponten and B. K. Siesjo. Gradients of CO_2 tension in the brain. *Acta Physiol. Scand.* **67**, 129–140 (1966).
12. M. Reivich. Arterial PCO_2 and cerebral hemodynamics. *Am. J. Physiol.* **206**, 25–35 (1964).
13. W. H. Press, B. P. Flannery, S. H. Teukolsky and W. T. Vetterling. *Numerical Recipes: The Art of Scientific Computing*. Cambridge University Press, Cambridge (1989).
14. J. P. Muizelaar. Cerebral blood flow, cerebral blood volume, and cerebral metabolism after severe head injury. In: *Textbook of Head Injury*, D. P. Becker and S. K. Gudemans (Eds), 221–240. Saunders, Philadelphia (1989).